PAPER

Check for updates

Highly sensitive turn-off fluorescent detection of cyanide in aqueous medium using dicyanovinyl-substituted phenanthridine fluorophore†

Saravanakumar Manickam and Sathiyanarayanan Kulathu Iyer [ID] *

Herein, the turn-off fluorescence sensor of 2-((4′-(7,8,13,14-tetrahydrodibenzo[a,i]phenanthridin-5-yl)-[1,1′-biphenyl]-4-yl)methylene)malononitrile (7) was developed for the recognition of CN⁻ ions and studied using different spectroscopic techniques. The selective recognition of CN⁻ ions by 7 was investigated *via* UV-vis spectroscopy and fluorescence studies in acetonitrile solvent, which exhibited an obvious color change from orange to colorless under 365 UV light. The sensor compound 7 possesses a high binding constant (K_a) for CN⁻ ions in the order of 5.22×10^6 M⁻¹. The results from the interference studies revealed that probe 7 shows high sensing selectivity and sensitivity for CN⁻ ions over other competitive anions. Probe 7 interacts with cyanide to form a 1 : 1 adduct, and this mechanism was further verified by ¹H NMR titration, Job's plot analyses and DFT studies. The sensor probe 7 exhibits advantages such as low limit of detection (LOD) of 39.3 nM, fast response and sensing in a wide pH range of 3 to 11. The practical application of 7 was successfully demonstrated for the determination of CN⁻ ions in test paper strips and various water samples.

Introduction

The cyanide anion plays an important role in medicine,[1] biology,[2] and catalysis;[3] however, it is considered as the most toxic anion in environmental chemistry.[4] The cyanide anion is a serious environmental pollutant, especially in natural water, soil and air, resulting from human activities.[5] Moreover, trace amounts of cyanide accumulate in animal and human bodies, which eventually results in death within a few minutes of intake because of its intense toxicity to physiological systems.[6] Cyanide is useful in various industrial fields[7] such as the synthesis of acrylic plastic,[8] synthetic fibers,[9] and resins[10] and the extraction of gold. However, these activities increase the contamination risk in the environment.[11] The World Health Organization (WHO) has set the standard limit of CN⁻ ions in potable water at 1.9 μM to prevent poisoning.[12] Hence, because of its toxicity and industrial functions, the highly sensitive and selective determination of CN⁻ ions at low levels is of considerable importance. Therefore, efficient methods for the sensitive and reliable detection of CN⁻ such as voltammetric, potentiometric, electrochemical and optical techniques have been developed.[13] Among the various traditional approaches, the optical technique using UV-vis and fluorescence spectroscopy has gained

increasing attention because of its outstanding properties such as high sensitivity and easy detection by the naked eye.

We are interested in designing and developing new dicyanovinyl-based phenanthridine systems containing phenanthridine as the receptor and the dicyanovinyl moiety as a chelator for CN⁻ ions. Accordingly, probe 7, not only acts as an electron-accepting group to induce intramolecular charge transfer (ICT) transitions, but also as a cyanide binding site due to is dicyanovinyl carbon. Thus far, various fluorescent sensor mechanisms for the recognition of cyanide ions have been developed, which include metal complex ensemble displacement,[14] electron deficient alkenes,[15] hydrogen bonding interaction with two proton donors,[16] supramolecular self-assembly,[17] excited-state ICT[18] and nucleophilic addition reaction.[19] Among them, the present receptor may exhibit nucleophilic addition reaction involving cyanide attack on the electron-deficient dicyanovinyl carbon for highly selective cyanide ion sensing and can effectively reduce the interference by other anions.

Herein, we report a new colorimetric and turn-off fluorescent sensor for CN⁻ ions in aqueous medium (probe 7, Scheme 1), which is based on the fast nucleophilic attack of cyanide anions on the dicyanovinyl carbon. Sensor probe 7 contains a conjugated phenanthridine moiety linked with a malononitrile group and has numerous benefits such as being highly reactive for cyanide anions with rapid response, good working pH range and distinct spectral changes (UV-vis and fluorescence spectra). The LOD of probe 7 was calculated using 3σ/slope[20] (linear plot of concentration of cyanide ions *versus* fluorescence intensity at

Department of Chemistry, School of Advanced Sciences, VIT University, Vellore-632014, India. E-mail: sathiya_kuna@hotmail.com

594 nm), which gave a value of about 39.3 nM, indicating that its LOD is well below the defined toxicity limit of the cyanide standard in drinking water set by the WHO (1.9 μM). To the best of our knowledge, no dicyanovinyl-appended tetrahydrodibenzo [*a,i*]phenanthridine-based chemosensor has been reported to date for the recognition of the CN⁻ anion. We also utilized sensor probe **7** for the detection of cyanide ion in real water samples and test paper strips.

Results and discussion

The synthetic procedure for compounds **5** and **7** is shown in Scheme 1. Aldehyde-substituted **5** and dicyanovinyl-substituted **7** were successively synthesized. The palladium-catalysed Suzuki coupling reaction was used to attach 4-formylphenyl boronic acid moieties to 4-bromosubstituted phenanthridine (**3**) to afford compound **5** with a yield of 64%. Subsequently, sensor probe **5** was further condensed with malononitrile using the piperidine-mediated Knoevenagel condensation reaction to convert the carbonyl group to the dicyanovinyl moiety of probe **7**. The receptor structures of compounds **5** and **7** were fully characterized *via* FTIR, NMR and HRMS spectroscopy (ESI, Fig. S2–S6†).

As noted in Fig. 1, compound **5** showed two absorption bands at 271 and 328 nm, giving a colorless solution in 20 μM of CH₃CN. Furthermore, compound **5** was condensed with malononitrile, and the resultant compound **7** exhibited three absorption bands centered at 267, 288 and 368 nm, which can be attributed to the π–π* and ICT transitions, giving a yellow solution in CH₃CN (20 μM). Upon the addition of 100 μL of CN⁻ to **7**, the ICT peak of **7** gradually decreased and a new absorption band appeared at 325 nm, which was the blue-shifted absorption band (**7 + CN⁻**). Meanwhile, the addition of 100 μL CN⁻ to **7** (594 nm) in CH₃CN significantly decreased its emission intensity, due to the nucleophilic reaction. The quantum yield of (Φ_{fl}) probe **7** was determined to be 21%, which was reduced substantially to 4% upon the addition of 12 equiv. of CN⁻ ions. This was determined using quinine sulphate as a standard (Φ_{fl} = 0.54 in 0.5 M conc. H₂SO₄).[21] The low Φ_{fl} of [**7 + CN⁻**] may be due to the blocked ICT transitions in the molecule (Table 1).
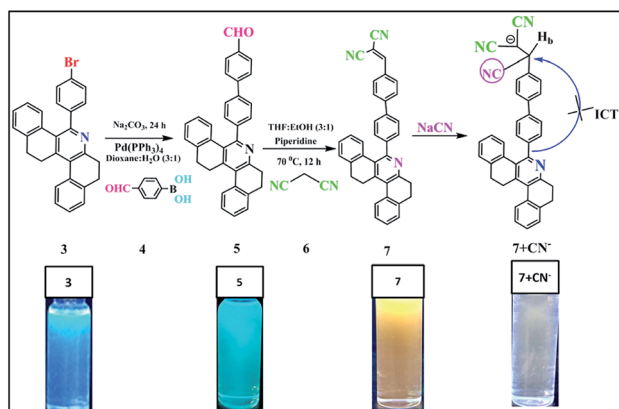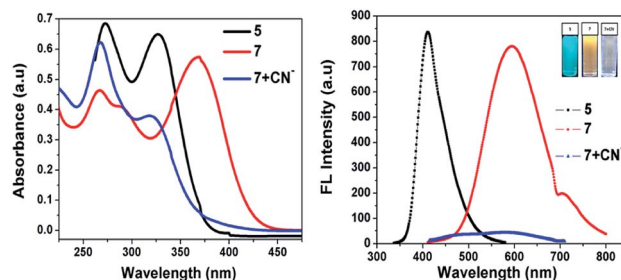

Fig. 1 Absorption (left) and fluorescence (right) spectra of **5** and **7** in the absence and presence of cyanide ions in acetonitrile.

Selectivity studies

Fig. 2 shows that almost no distinct change was found in the UV-vis absorption and emission spectrum of compound **7** (20 μM in acetonitrile) upon the addition of 100 μL of other anions such as F⁻, Cl⁻, OH⁻, CH₃COO⁻, CO₃²⁻, S₂O₃⁻, HCO₃²⁻, SO₄⁻ and PO₄³⁻ (1 mM in aqueous medium). Considering the acceptor group of the dicyanovinyl moiety of **7**, an aqueous medium of anions at same concentration was used. In the case of the CN⁻ ion, owing to its higher nucleophilicity compared to the other anions, the solution color of sensor probe **7** quickly changed from orange to colorless under a UV lamp at 365 nm, while no color changes occurred in the solutions with the other anions. This is due to the interaction of cyanide ion with the dicyanovinyl group of **7**, which was reduced, and hence quenching of the emission was observed. Its selectivity for CN⁻ was further investigated by UV-vis absorption and fluorescence titration experiments.

UV-vis spectroscopic studies

The UV-vis absorption spectrum of **7** showed a characteristic absorption band at 375 nm together with two shoulder absorption signals at 270 nm and 298 nm. Upon the addition of CN⁻ to the acetonitrile solution of **7**, the absorption maximum peak at 375 nm, which is attributed to ICT transitions, gradually decreased and a new band appeared at 325 nm. This hypsochromic shift with clear isosbestic point at 338 nm supports the occurrence of a new cyanide adduct product. This suggests that CN⁻ must undergo 1 : 1 stoichiometric complexation with the formation of a CN⁻ adduct. The linear calibration plot of the absorbance at 375 nm *versus* concentration of CN⁻ ions presents evidence for the changes in the absorption spectrum. Moreover, the color of the solution of [**7 + CN⁻**] turned almost colorless, which was clearly visualized by the naked eye, indicating the formation of a new CN⁻ adduct species through the favorable nucleophilic attack of CN⁻ on the dicyanovinyl carbon (Fig. 3).

Fluorescence spectroscopic studies

The binding mechanism properties of **7** (20 μM in acetonitrile) towards CN⁻ ions (1 mM in aqueous medium) was also investigated *via* a fluorescence titration experiment, and the results are shown in Fig. 4. The free sensor compound **7** showed a very

Scheme 1 Structure of compound **7** and its sensing mechanism.

Table 1 Optical properties of compounds **5** and **7** in acetonitrile solution

Probe	$\lambda_{max}{}^a$ [nm]	$F_{max}{}^b$ [nm] solution	$\Delta_{ss}{}^c$ (cm^{-1})	$\Phi_{fl}{}^d$	Binding constant (M^{-1})
7	267, 288, 368	594	10 338	0.21	—
7 + CN$^-$	276, 325	580	13 527	0.04	5.22×10^6 M^{-1}

[a] Measured at a concentration of 2×10^{-5} M. [b] The excitation wavelength was 370 nm. [c] Stokes shift = UV–FL. [d] Absolute quantum yield was measured in CH$_3$CN solvent using quinine sulfate as the standard (Φ_{fl} = 0.54 in 0.5 M conc. H$_2$SO$_4$).
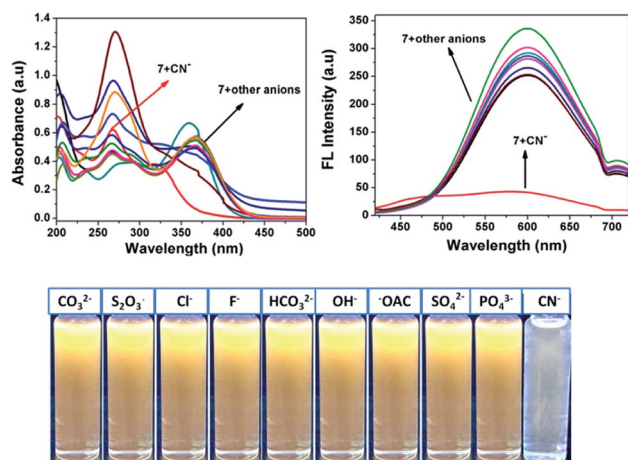

Fig. 2 Absorption (left) and fluorescence (right) spectral changes of **7** upon the addition of one equivalent of various anions in acetonitrile medium.

high fluorescence peak at 594 nm upon excitation at 370 nm, the emission intensity of which decreased gradually with the addition of CN$^-$ ions and became saturated with 12 equiv. of CN$^-$, which may be due to the formation of the cyanide adduct between **7** and CN$^-$ ions *via* nucleophilic addition of CN$^-$ to the C=C double bond of the malononitrile unit. As expected, the emission peak of compound **7** at 594 nm disappeared completely with a gradual increase in the concentration of cyanide (0 to 12 equiv.) in aqueous media. Meanwhile, a dramatic color change from orange to colorless was easily detected by UV light.

Furthermore, a liner plot between the fluorescence intensity at 594 nm *versus* the concentration of CN$^-$ was obtained over

the range of 2 to 5 μM (Fig. 4, right). The LOD was calculated using 3σ/slope, where σ represents the standard deviation of 10 blank probe samples and the slope is from the linear plot. The detection limit was calculated from the fluorescence titrations and the detection limit of **7** for CN$^-$ ions was found to be as low as 39.3 nM, suggesting that the sensor probe **7** has great potential to detect CN$^-$ ions in drinking water. Moreover, the limit of detection of the present sensor **7** is remarkable compared to that of recent sensors reported in the literature, as shown in ESI Table S1.†[22]

The stoichiometric interaction between **7** with CN$^-$ ions was determined by employing Job's plot analysis. The curve with a maximum at 0.5 mole fraction in the Job's plot experiment indicates the possible formation of a 1 : 1 complex between sensor probe **7** and CN$^-$ ions (Fig. 5, right). This is obvious based on the nucleophilic attack of cyanide on the dicyanovinyl carbon to produce [**7 + CN$^-$**]. Thus, the Benesi–Hildebrand analysis plot was obtained based on the 1 : 1 binding model between **7** and CN$^-$ with the formation of [**7 + CN$^-$**]. From the emission quenching spectra, the association binding constant for the formation of the [**7 + CN$^-$**] adduct was determined to be 5.22×10^{-6} M^{-1} according to the Benesi–Hildebrand equation (Fig. 5, left).

Interference study and pH effect

Interference studies were also performed to investigate the emission spectral changes for probe **7** upon CN$^-$ detection. Upon the addition of cyanide ions to the sensor **7** solution, the emission intensity of the mixture at 594 nm decreased gradually, and there was no apparent color change in the solution or significant fluorescence variation in the presence of other anions (F$^-$, Cl$^-$, OH$^-$, CH$_3$COO$^-$, CO$_3{}^{2-}$, S$_2$O$_3{}^-$, HCO$_3{}^{2-}$, SO$_4$
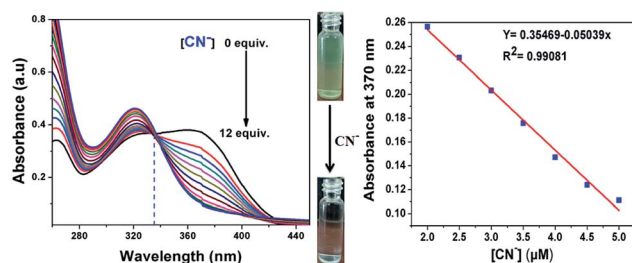

Fig. 3 Absorption spectra changes of probe **7** upon the addition of different concentrations of CN$^-$ in acetonitrile (left) and the linear calibration curve of the absorbance at 375 nm *versus* concentration of CN$^-$ in the range of 2 to 5 μM (right).
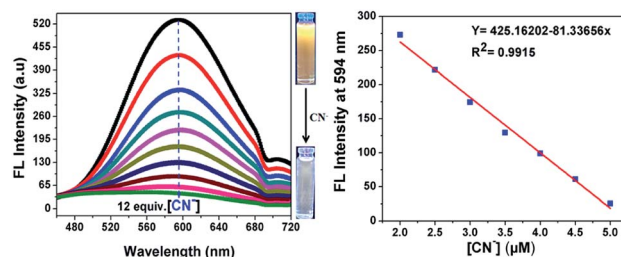

Fig. 4 Fluorescence spectra changes of probe **7** in acetonitrile upon the addition of different concentrations of aqueous CN$^-$ anion upon excitation at 370 nm (left) and a linear calibration curve of the emission band intensity at 594 nm *versus* concentration of CN$^-$ in the range of 2 to 5 μM (right).
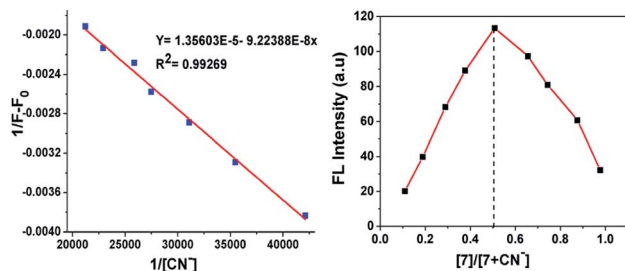
Fig. 5 Benesi–Hildebrand plot of fluorescence intensity at 594 nm (left) and Job's plot complexation between **7** and CN^- (right).

Fig. 7 Effect of response time on fluorescence intensity of sensor probe **7** (20 μM) in the presence of CN^- ions (3.0 equiv.).

and PO_4^{3-}), as shown in Fig. 6. These investigations indicate that the binding interaction between compound **7** and CN^- is stronger than that between **7** and other anions. Therefore, compound **7** can act as a highly selective and as specific turn-off fluorescence sensor for the cyanide anion even in the presence of other competitive anions without any interference.

The pH-dependence of the emission intensity changes of probe **7** alone and the turn-off sensor [**7** + **CN**$^-$] adduct was examined over a wide pH range of 1 to 11 (Fig. 6, right). The results show that fluorescence of **7** exhibited a strong emission but emission intensity changes were not observed in the pH range of 1 to 3. Above pH 4.0, the fluorescence intensity gradually increased, which may be due to ICT in the excited state. In the presence of 50 equiv. of **CN**$^-$, the fluorescence intensity the solution of [**7** + **CN**$^-$] remained unchanged up to a pH of 2.0, but it increased from pH 3 to 11 due to the protonation of the CN^- ion. These results reiterate that probe **7** is suitable for CN^- detection in the broad pH range of 3 to 11, especially at near neutral pH conditions.

Effect of response time

To investigate the complex formation ability of CN^- by sensor **7**, we explored the effect of the response time on its fluorescence intensity for the detection of CN^-. As displayed in Fig. 7, the fluorescence emission intensity at 594 nm of probe **7** instantly decreased and was completely quenched within 20 s and stabilized thereafter, suggesting that the reaction system was very fast. This suggests that probe **7** can be used as an effective tool for the real-time sensing of CN^-.[23]
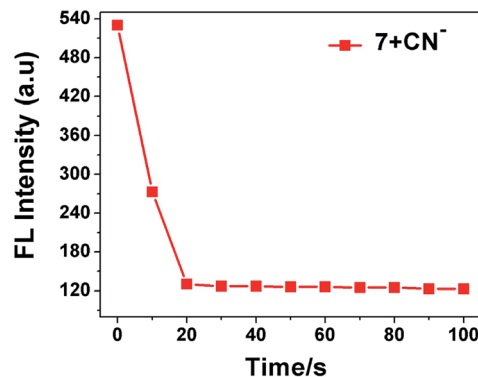
Electrochemical studies

To substantiate the electrochemical behaviour of **7** in the absence and presence of different concentrations of cyanide ions, CN^- concentrations in the range of 10 to 40 μL were investigated. We carried out differential pulse voltammetry (DPV) with **7** in acetonitrile containing 0.1 M $TBAFP_6$ as the supporting electrolyte, as visualized in Fig. 8. Compound **7** exhibited a typical voltammogram for the electroreduction of the dicyanovinyl moiety with a reduction peak at −1.41 eV. As noted from the voltammograms, the progressive addition of cyanide ions to the solution of **7** resulted in a significant reduction peak, which was shifted to a less negative reduction potential with a concurrent decrease in the current intensity. The reduction peak was shifted from a higher to lower negative potential (−1.41 eV, −1.27 eV, −1.16 eV and −1.07 eV), corresponding to the formation of the [**7** + **CN**$^-$] adduct. This is due to the fact that the cyanide sensing mechanism involves a turn-off ICT transition between the electron-donor pyridine ring and electron-acceptor dicyanovinyl group in the probe **7** molecule. The obtained results clearly demonstrated that the negative charge was generated on the C-atom in the dicyanovinyl moiety, which was further confirmed by the NMR spectral analysis.[24]

Mechanism studies

^{1}H NMR titration was further employed to investigate the potential interaction mechanisms of probe **7** and cyanide anions. To demonstrate the reaction process, ^{1}H NMR titration
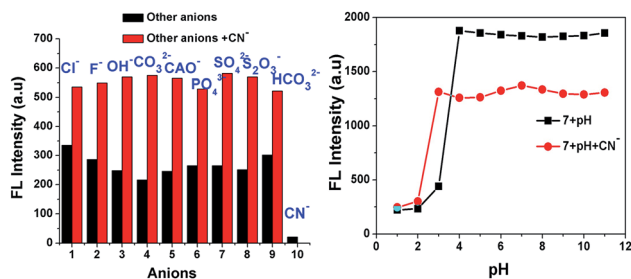

Fig. 6 Fluorescence intensity of **7** at 594 nm upon the addition of anions and also cyanide with other interfering anions (left) and pH effect of **7** and [**7** + **CN**$^-$] (right).
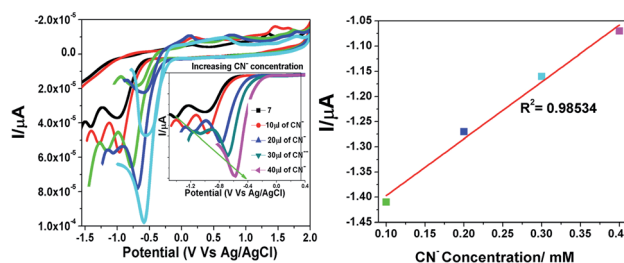

Fig. 8 Changes in the redox potential of **7** in the presence of different concentrations of cyanide in acetonitrile.

of **7** with different concentrations of cyanide anion (as NaCN, 0 to 0.5 equiv.) was also performed in DMSO-d_6 (Fig. 9). Ligand **7** alone exhibited singlet peaks at 8.6 ppm, which were assigned to the H_a protons. After the addition of CN^- to the solution of **7**, the singlet at 8.6 ppm (H_a), corresponding to the signal of the dicyanovinyl group, clearly shifted from downfield to upfield, which indicates that the C=C double bond gradually disappeared. When 0.6 equiv. of CN^- was added, the singlet peaks corresponding to the H_a protons completely disappeared, and simultaneously a new singlet peak developed at 4.7 ppm (H_b), which can be attributed to the formation of cyanohydrin [**7** + CN^-]. These observations clearly confirmed the Michael addition reaction between **7** and CN^-, and their conversion into cyanohydrin. Additionally, the FTIR and HRMS spectra of probe **7** upon the addition of CN^- confirmed the formation of the [**7** + CN^-] adduct, where the peak at m/z 537.2083 is assigned to the negatively charged species of [**7** + CN^-] (Fig. S1 and S7†).

Practical application

To elucidate the practical applicability of **7** for the detection of CN^-, easy to use test paper kits were prepared by immersing Whatman filter paper strips in the acetonitrile solution of **7** and then drying them in air for 30 min. Solutions with various cyanide concentrations were prepared in HPLC-grade H_2O by dissolving the required quantity of sodium cyanide. As presented in Fig. 10, the coated paper strips, when immersed in 0 to 12 equiv. of cyanide ion solution, immediately changed from green to colorless under illumination at 365 nm with a portable UV light and could be visually seen also. This indicates that compound **7** can be made into ready to use test paper to detect cyanide ions in natural water with high selectivity for real-time application.[25]
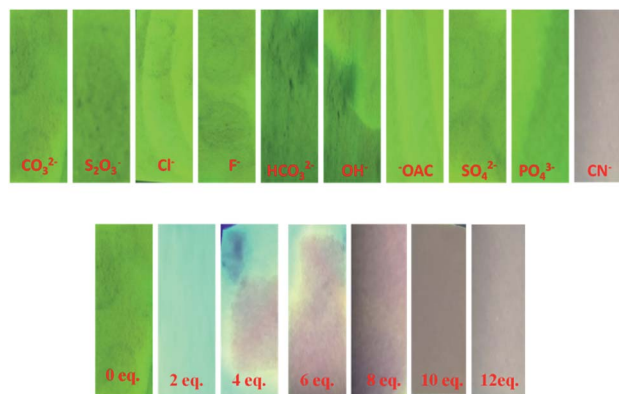

Fig. 10 Fluorescence color changes of the test paper of **7** upon the addition of cyanide ion solution in aqueous medium and the test paper strips were irradiated under a UV lamp at 365 nm.

Real sample analysis

To demonstrate the practical utility of probe **7** with increasing concentrations of CN^- in environmental water samples, an experiment was performed using different water samples such as distilled water, tap water and lake water. The different water samples were collected from the Vellore region (VIT Institute, TN, and India) and checked for CN^-. After preparing 10 μM, 20 μM and 30 μM of cyanide ions in the water samples, the experiment was repeated 3 times for each sample, and the results are shown in Fig. 11. The emission response of probe **7** for the detection of CN^- in tap water and lake water was in good agreement with that in the distilled water, which showed the formation of the [**7** + CN^-] complex. This result confirms that probe **7** as a CN^- sensing platform has great potential for the determination of cyanide ions in environmental water samples.[26]

Molecular logic gate operations

The quenching fluorescence intensity process of sensor **7** can be represented by a molecular "INHIBIT" logic gate, employing **7** (input 1) and CN^- (input 2) as the inputs and considering the fluorescence intensity at around 594 nm as the output signal. The corresponding truth table values are given in Fig. 12c. In this regard, when sensor **7** was present (input 1), the emission was "1", which represented the "ON" state. The introduction of
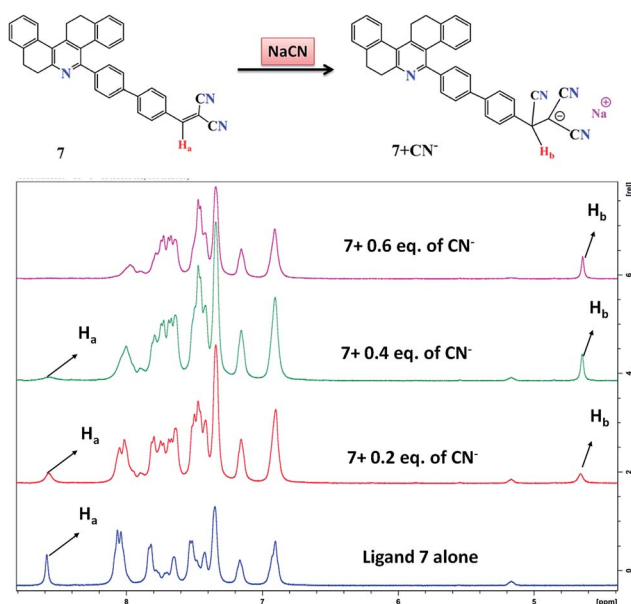

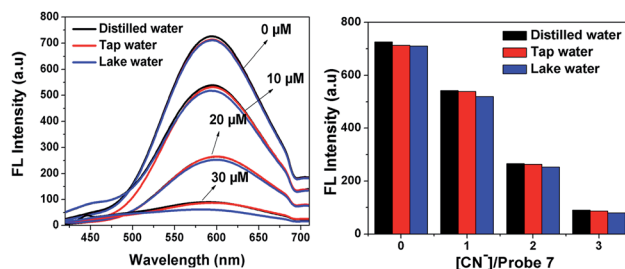**Fig. 9** ^{1}H NMR titrations of probe **7** with different concentrations of NaCN in DMSO-d_6.

Fig. 11 Fluorescence detection of different concentrations of CN^- in distilled water, tap water and lake water by probe **7** (20 μM).
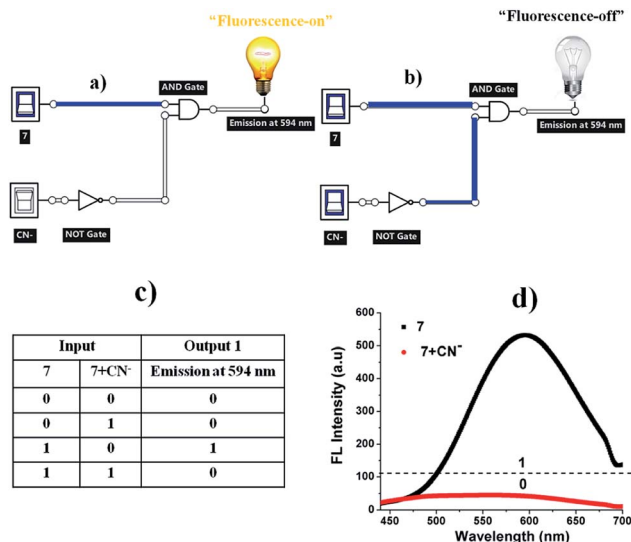
Fig. 12 (a) "Fluorescence-on" and (b) "fluorescence-off" logic circuit for 7 and 7 + CN⁻. (c) Corresponding truth table and (d) fluorescence spectra of 7 in the presence of CN⁻ (12 equiv.).

CN⁻ to sensor system 7 provided the output logic values of "1", where "1" represents the "ON" and "OFF" states (Fig. 12d). In this case, CN⁻ induced a decrease in the emission band at 594 nm, exhibiting OFF behaviour. Therefore, the fluorescence intensity at 594 nm was construed to be in the "ON" state (7) while the weak fluorescence intensity was considered as the "OFF" state (7 + **CN⁻**).[27]

Molecular orbital calculation

To further correlate the electronic structure of sensor probes 7 and 7 + **CN⁻**, theoretical optimization and calculation were performed using the density functional theory (DFT) with the B3LYP functional, employing the 6-331G (d, p) basis set, as implemented in the Gaussian 09 program.[28] The optimized structure and calculated HOMO and LUMO values in the frontier molecular orbitals of 7 and 7 + **CN⁻** are presented in Fig. 13 and 14, respectively. For compound 7, the electron density in the HOMO is located on the phenanthridine skeleton, while that of the LUMO is distributed on the biphenyl malononitrile moiety. In terms of the adduct 7 + **CN⁻**, the π-electron of HOMO is mainly situated on the dicyanovinyl unit and LUMO spread over the phenanthridine ring. Thus, in comparison with 7, the distribution of the HOMO and LUMO is entirely different in 7 +
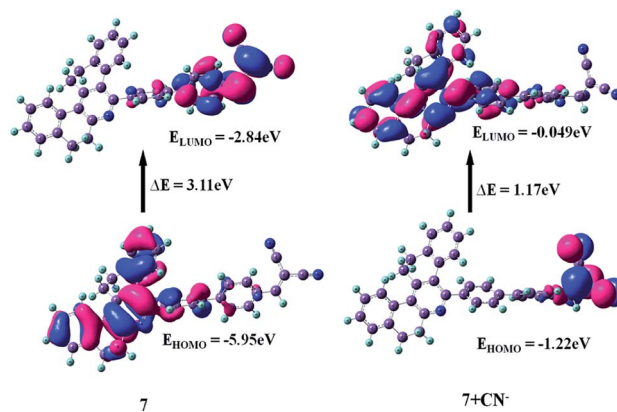

Fig. 13 Optimized structures of 7 and 7 + CN⁻.

Fig. 14 HOMO and LUMO energy levels of 7 and 7 + CN⁻.

CN⁻, which is due to the reaction with the cyanide ion, and thus the 7 + **CN⁻** adduct was observed. This involves the removal of the strong electron-deficient malononitrile group, which leads to the ICT transitions being diminished.

The energy gaps between the HOMO and LUMO level of 7 and 7 + **CN⁻** are 3.11 eV and 1.17 eV, respectively, indicating the turn-off fluorescence after the formation of the adduct. The calculated energy gap value of 7 + **CN⁻** (1.17 eV) is much lower than that of 7 (3.11 eV). Therefore, the DFT results suggest that the interaction of the CN⁻ ion with 7 effectively reduces the HOMO–LUMO energy gap of the 7 + **CN⁻** adduct and stabilizes the system. In addition, the time-dependent DFT (TDDFT) calculated electronic absorptions of 7 and 7 + **CN⁻** are 365 nm and 332 nm, which are comparable to the experimentally measured results (368 and 320 nm), respectively. This is in good agreement with the experimental results (ESI, Table S2†).

Conclusion

In this study, we successfully designed and synthesized a dicyanovinyl-attached phenanthridine moiety *via* the Knoevenagel condensation method, which was well characterized *via* numerous spectroscopic techniques. Sensor compound 7 for CN⁻ sensing was investigated based on UV-vis and fluorescence methods, and electrochemical and theoretical calculations. Fluorescence turn-off was observed for 7 upon the addition of CN⁻ at the bridging dicyanovinyl bond with an obvious color change, which was clearly visible by the naked eye. The B–H plot and Job's plot results clearly indicate that the binding constant of [7 + **CN⁻**] is 5.22×10^6 M⁻¹ and the mole fraction is 0.5, indicating a 1 : 1 stoichiometric complexation reaction between 7 and CN⁻ ions. The LOD was determined to be 39.3 nM, which is much lower than the WHO (1.9 μM) agency standard for drinking water. The pH studies revealed that sensor compound 7 works well in the pH range of 3–11. The ¹H NMR titration and Job's plot analyses suggest that the cyanide ion attacks the C=C double bond of the phenanthridine dicyanovinyl moiety and converts it into a cyanide adduct. Therefore, sensor probe 7 can be utilized successfully for the determination of cyanide ions in
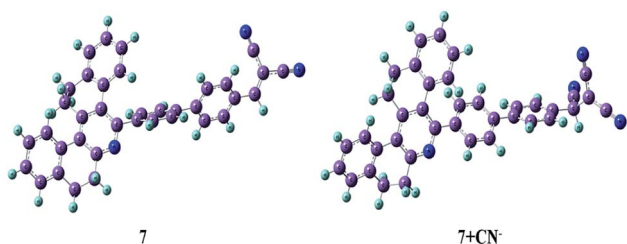
paper strips for practical application and also in environmental water samples.

Experimental

General experimental

Chemicals such as 2-tetralone, 4-bromobenzaldehyde, 4-formylphenyl boronic acid, malononitrile and $Pd(PPh_3)_4$ catalyst were obtained commercially from Alfa Aesar, Sigma Aldrich and Avra. Column chromatography was performed using silica with a mesh of 60–120. All organic solvents were of analytical grade and distilled before use. The sodium salts (F^-, Cl^-, OH^-, CH_3COO^-, CO_3^{2-}, $S_2O_3^-$, HCO_3^{2-}, CN^-, SO^{4-} and PO_4^{3-}) were purchased from TCI chemicals and used as received. ^1H NMR and ^{13}C NMR spectra were recorded in $CDCl_3$ using a Bruker 400 MHz instrument and TMS as the standard. HRMS spectra were measured on a Q-Tof mass analyzer. FTIR spectra of the solid compounds were measured on a Jasco-4100 spectrometer. UV-vis absorption and emission spectra were obtained on a Hitachi U-2910 spectrophotometer and Hitachi F-7000 fluorescence spectrometer using a 3 cm standard quartz cell, respectively. Fluorescence lifetime measurements were performed with the time-correlated single photon counting method setup using a nano LED as the excitation source. Electrochemical measurements were performed on a CH instrument (CH620E). A three-electrode configuration was used, which consisted of glassy carbon (working electrode), platinum wire (auxiliary electrode) and saturated calomel electrodes (reference electrode). Experiments were performed in dry acetonitrile solvent and 0.1 M of tetrabutylammonium hexafluorophosphate as the supporting electrolyte.

Procedure for CN^- sensing

Stock solutions of probe 7 (20 μM) and all the anions (1 mM) were prepared in CH_3CN and analytical grade pure water. UV-vis absorption and emission titration experiments were carried out with 20 μM of probe 7 against 1 mM of various anions at 25 °C.

Synthesis of probe 3

5-(4-Bromophenyl)-7,8,13,14-tetrahydrodibenzo[a,i]phenanthridine (3) was prepared according to our previously reported procedure.[29]

Synthesis of probe 5

500 mg (1 mmol) of compound 3, 160 mg (1.2 mmol) of 4-formylphenylboronic acid 4 and 300 mg of Na_2CO_3 (2.5 mmol) and then $Pd(PPh_3)_4$ (127 mg, 10 mol%) were dissolved in 5 mL of 1,4-dioxane/H_2O (4 : 1) mixture at room temperature and then stirred for 5 min. The reaction system was heated at 80 °C for an additional 12 h under nitrogen atmosphere with stirring continued until TLC revealed that the reaction was completed. Then, the reaction vessel was allowed to cool to room temperature and the crude residue was purified by column chromatography (silica) using n-hexane/ethyl acetate (8 : 2) as the eluent to afford probe 5 as a white solid.

Synthesis of probe 7

Compound 5 (210 mg, 1 mmol) and malononitrile 6 (2 mmol) were added to absolute ethanol (8 mL) and tetrahydrofuran (5 mL), and 10 μL of piperidine was added to the solution. The reaction mixture was then heated and stirred at 75 °C for 12 h. Upon cooling to room temperature, the reaction mixture was monitored by TLC analysis. The solvent was rotary evaporated to dryness under vacuum. Subsequently, the yellow solid product was obtained after silica column chromatography with a mixture of 7 : 3 n-hexane/ethyl acetate as the eluent.

Compound 5

Yield 72% (365 mg), white solid. Melting point: 222–224 °C; IR (KBr): 406.98, 484.13, 621.08, 736.81, 761.88, 802.39, 821.68, 894.97, 943.19, 1001.16, 1031.92, 1111.00, 1170.79, 1219.01, 1286.52, 1392.61, 1429.25, 1548.84, 1600.92, 1695.43, 2837.29, 2943.37, 3032.10 cm^{-1}. ^1H NMR (400 MHz, $CDCl_3$) TM ppm δ: 2.79–2.80 (t, $J = 4$ Hz 2H, CH_2), 2.95–2.97 (t, $J = 8$ Hz 2H, CH_2), 3.13–3.11 (q, $J = 8$ Hz 2H, CH_2), 3.18–3.17 (t, $J = 4$ Hz 2H, CH_2), 6.95–6.93 (t, $J = 8$ Hz 1H, ArCH), 7.00–6.98 (d, $J = 8$ Hz 1H, ArCH), 7.17–7.15 (t, $J = 8$ Hz 1H, ArCH), 7.38–7.26 (m, 4H, ArCH), 7.55–7.54 (t, $J = 4$ Hz 1H, ArCH), 7.64–7.62 (q, $J = 8$ Hz 4H, ArCH), 7.80–7.78 (d, $J = 8$ Hz 2H, ArCH), 7.97–7.95 (d, $J = 8$ Hz 2H, ArCH), 10.06 (s, 1H, ArCHO); $^{13}C\{^1H\}$ NMR (100 MHz, $CDCl_3$) TM ppm: 29.2 (CH), 29.4 (CH), 29.5 (CH), 33.2 (CH), 125.7 (2 × CH), 126.1 (2 × CH), 127.0 (2 × CH), 127.1 (2 × CH), 127.3 (CH), 127.6 (CH), 127.7 (CH), 127.8 (CH), 127.9 (CH), 128.7 (C), 129.0 (CH), 129.6 (CH), 130.3 (CH), 130.5 (C), 132.8 (C), 132.9 (C), 135.1 (C), 138.7 (C), 138.9 (C), 139.7 (C), 142.3 (C), 145.8 (C), 146.9 (C), 153.0 (C), 158.3 (C), 191.9 (CH). HRMS (Quadrupole) for $C_{34}H_{25}NO$ calculated $[M^+]$ m/z 463.1936, found 463.1933.

Compound 7

Yield 68% (157 mg), yellow solid. Melting point: 242–244 °C; IR (KBr): 482.20, 615.29, 744.52, 804.32, 825.53, 925.53, 1001.06, 1112.93, 1197.79, 1224.80, 1288.45, 1394.53, 1423.47, 1544.98, 1579.70, 1695.43, 2223.92, 2839.22, 2939.52 cm^{-1}. ^1H NMR (400 MHz, $CDCl_3$) TM ppm: 2.79–2.80 (t, $J = 4$ Hz 2H, CH_2), 2.95–2.97 (t, $J = 8$ Hz 2H, CH_2), 3.12–3.10 (q, $J = 8$ Hz 2H, CH_2), 3.18–3.17 (t, $J = 4$ Hz 2H, CH_2), 6.94–6.92 (t, $J = 8$ Hz 1H, ArCH), 6.99–6.97 (d, $J = 8$ Hz 1H, ArCH), 7.18–7.16 (t, $J = 8$ Hz 1H, ArCH), 7.38–7.17 (m, 4H, ArCH), 7.54–7.53 (t, $J = 4$ Hz 1H, ArCH), 7.61–7.59 (q, $J = 8$ Hz 4H, ArCH), 7.81–7.79 (d, $J = 8$ Hz 3H, ArCH), 8.00–7.98 (d, $J = 8$ Hz 2H, ArCH); $^{13}C\{^1H\}$ NMR (100 MHz, $CDCl_3$) TM ppm: 29.2 (CH), 29.4 (CH), 29.5 (CH), 33.1 (CH), 81.8 (C), 112.8 (CN), 113.9 (CN), 125.8 (2 × CH), 126.1 (2 × CH), 127.1 (CH), 127.2 (CH), 127.8 (CH), 127.9 (CH), 128.7 (C), 129.0 (2 × CH), 129.6 (CH), 129.8 (CH), 130.7 (2 × CH), 131.4 (2 × CH), 132.8 (2 × C), 132.9 (C), 138.0 (2 × C), 138.8 (C), 139.6 (C), 142.9 (C), 145.8 (C), 147.0 (C), 152.8 (C), 158.3 (C), 159.2 (CH). HRMS (Quadrupole) for $C_{37}H_{25}N_3$ calculated $[M^+]$ m/z 511.2048, found 511.2045.

Conflicts of interest

There is no conflict of interest.

Acknowledgements

References

1 (a) P. D. Beer and P. A. Gale, *Angew. Chem., Int. Ed.*, 2001, **40**, 486–516; (b) G. Zoppellaro, V. Enkelmann, A. Geies and M. Baumgarten, *Org. Lett.*, 2004, **6**, 4929–4932.

2 (a) D. G. Cho and J. L. Sessler, *Chem. Soc. Rev.*, 2009, **38**, 1647–1662; (b) Z. Xu, S. K. Kim and J. Yoon, *Chem. Soc. Rev.*, 2010, **39**, 1457–1466.

3 (a) R. M. Duke, E. B. Veale, F. M. Pfeffer, P. E. Kruger and T. Gunnlaugsson, *Chem. Soc. Rev.*, 2010, **39**, 3936–3953; (b) S. Fustero, R. Román, J. F. Sanz-Cervera, A. Simón-Fuentes, J. Bueno and S. Villanova, *J. Org. Chem.*, 2008, **73**, 8545–8552.

4 (a) K. R. Dey, B. M. Wong and M. A. Hossain, *Tetrahedron Lett.*, 2010, **51**, 1329–1332; (b) Z. Xu, X. Chen, H. N. Kim and J. Yoon, *Chem. Soc. Rev.*, 2010, **39**, 127–137; (c) W.-J. Qu, W.-T. Li, H.-L. Zhang, T.-B. Wei, Q. Lin, H. Yao and Y.-M. Zhang, *J. Heterocycl. Chem.*, 2018, **55**, 879–887; (d) W.-j. Qu, G.-y. Gao, B.-b. Shi, T.-b. Wei, Y.-m. Zhang, Q. Lin and H. Yao, *Sens. Actuators, B*, 2014, **204**, 368–374; (e) W.-J. Qu, W.-T. Li, H.-L. Zhang, T.-B. Wei, Q. Lin, H. Yao and Y.-M. Zhang, *Sens. Actuators, B*, 2017, **241**, 430–437.

5 (a) C. Brugnara, *Clin. Chem.*, 2003, **49**, 1573; (b) L. Nelson, *J. Emerg. Nurs.*, 2006, **32**, S8–S11.

6 (a) J. D. Johnson, T. L. Meisenheimer and G. E. Isom, *Toxicol. Appl. Pharmacol.*, 1986, **84**, 464–469; (b) C. Y. Kim, S. Park and H.-J. Kim, *Dyes Pigm.*, 2016, **130**, 251–255; (c) E. V. Brouillet, A. R. Kennedy, K. Koszinowski, R. McLellan, R. E. Mulvey and S. D. Robertson, *Dalton Trans.*, 2016, **45**, 5590–5597.

7 D. T. Thompson, *Gold Bull.*, 2001, **34**, 133.

8 P. Pary, J. F. Bengoa, M. S. Conconi, S. Bruno, M. Zapponi and W. A. Egli, *Trans. IMF*, 2017, **95**, 83–89.

9 O. A. A. Eletta, O. A. Ajayi, O. O. Ogunleye and I. C. Akpan, *J. Environ. Chem. Eng.*, 2016, **4**, 1367–1375.

10 T. Gunnlaugsson, M. Glynn, G. M. Tocci, P. E. Kruger and F. M. Pfeffer, *Coord. Chem. Rev.*, 2006, **250**, 3094–3117.

11 (a) D. S. Kim, Y. M. Chung, M. Jun and K. H. Ahn, *J. Org. Chem.*, 2009, **74**, 4849–4854; (b) Y. C. Yang, J. A. Baker and J. R. Ward, *Chem. Rev.*, 1992, **92**, 1729–1743.

12 (a) W. H. Organization, *Guidelines For Drinking-Water Quality*, 1996; (b) World Health Organization, *Guidelines for Drinking-Water Quality*, World Health Organization, 3rd edn, Geneva, 2008, p. 188.

13 (a) T. Suzuki, A. Hioki and M. Kurahashi, *Anal. Chim. Acta*, 2003, **476**, 159–165; (b) D. Shan, C. Mousty and S. Cosnier, *Anal. Chem.*, 2004, **76**, 178–183; (c) A. Afkhami, N. Sarlak and A. R. Zarei, *Talanta*, 2007, **71**, 893–899; (d) A. Safavi, N. Maleki and H. R. Shahbaazi, *Anal. Chim. Acta*, 2004,

503, 213–221; (e) B. Desharnais, G. Huppé, M. Lamarche, P. Mireault and C. D. Skinner, *Forensic Sci. Int.*, 2012, **222**, 346–351; (f) H. Sulistyarti and S. D. Kolev, *Microchem. J.*, 2013, **111**, 103–107.

14 (a) X. Lou, D. Ou, Q. Li and Z. Li, *Chem. Commun.*, 2012, **48**, 8462–8477; (b) Y. Y. Guo, X. L. Tang, F. P. Hou, J. Wu, W. Dou, W. W. Qin, J. X. Ru, G. L. Zhang, W. S. Liu and X. J. Yao, *Sens. Actuators, B*, 2013, **181**, 202–208.

15 (a) S. Kumar, P. Singh, G. Hundal, M. Singh Hundal and S. Kumar, *Chem. Commun.*, 2013, **49**, 2667–2669; (b) X. B. Cheng, H. Li, F. Zheng, Q. Lin, H. Yao, Y. M. Zhang and T. B. Wei, *RSC Adv.*, 2016, **6**, 27130–27135.

16 (a) L. Yang, X. Li, Y. Qu, W. Qu, X. Zhang, Y. Hang, H. Ågren and J. Hua, *Sens. Actuators, B*, 2014, **203**, 833–847; (b) Y. Shiraishi, M. Nakamura, N. Hayashi and T. Hirai, *Anal. Chem.*, 2016, **88**, 6805–6811.

17 H. L. Zhang, T. B. Wei, W. T. Li, W. J. Qu, Y. L. Leng, J. H. Zhang, Q. Lin, Y. M. Zhang and H. Yao, *Spectrochim. Acta, Part A*, 2017, **175**, 117–124.

18 (a) A. C. Sedgwick, L. Wu, H.-H. Han, S. D. Bull, X.-P. He, T. D. James, J. L. Sessler, B. Z. Tang, H. Tian and J. Yoon, *Chem. Soc. Rev.*, 2018, **47**, 8842–8880; (b) C. Rao, Z. Wang, Z. Li, L. Chen, C. Fu, T. Zhu, X. Chen, Z. Wang and C. Liu, *Analyst*, 2020, **145**, 1062–1068.

19 (a) P. Jayasudha, R. Manivannan and K. P. Elango, *Sens. Actuators, B*, 2017, **251**, 380–388; (b) T. Liu, X. Liu, M. A. Valencia, B. Sui, Y. Zhang and K. D. Belfield, *Eur. J. Org. Chem.*, 2017, **2017**, 3957–3964; (c) D. Y. Lee, N. Singh, A. Satyender and D. O. Jang, *Tetrahedron Lett.*, 2011, **52**, 6919–6922.

20 (a) J. Orrego-Hernández, N. Nuñez-Dallos and J. Portilla, *Talanta*, 2016, **152**, 432–437; (b) K. Aich, S. Goswami, S. Das and C. D. Mukhopadhyay, *RSC Adv.*, 2015, **5**, 31189–31194.

21 W. H. Melhuish, *J. Phys. Chem.*, 1961, **65**, 229–235.

22 (a) Y. Ding, T. Li, W. Zhu and Y. Xie, *Org. Biomol. Chem.*, 2012, **10**, 4201–4207; (b) S. Goswami, S. Paul and A. Manna, *Dalton Trans.*, 2013, **42**, 10682–10686; (c) R. K. Konidena and K. R. J. Thomas, *RSC Adv.*, 2014, **4**, 22902–22910; (d) Y. Zhang, D. Li, Y. Li and J. Yu, *Chem. Sci.*, 2014, **5**, 2710–2716; (e) W. Zheng, X. He, H. Chen, Y. Gao and H. Li, *Spectrochim. Acta, Part A*, 2014, **124**, 97–101; (f) J. Orrego-Hernández and J. Portilla, *J. Org. Chem.*, 2017, **82**, 13376–13385; (g) Q. Zou, F. Tao, H. Wu, W. W. Yu, T. Li and Y. Cui, *Dyes Pigm.*, 2019, **164**, 165–173; (h) Y.-X. Hua, Y. Shao, Y.-W. Wang and Y. Peng, *J. Org. Chem.*, 2017, **82**, 6259–6267; (i) E. Thanayupong, K. Suttisintong, M. Sukwattanasinitt and N. Niamnont, *New J. Chem.*, 2017, **41**, 4058–4064; (j) Q. Lin, X. Liu, T.-B. Wei and Y.-M. Zhang, *Chem.–Asian J.*, 2013, **8**, 3015–3021; (k) Q. Lin, T.-T. Lu, X. Zhu, T.-B. Wei, H. Li and Y.-M. Zhang, *Chem. Sci.*, 2016, **7**, 5341–5346; (l) J. Liu, Y.-Q. Fan, S.-S. Song, G.-F. Gong, J. Wang, X.-W. Guan, H. Yao, Y.-M. Zhang, T.-B. Wei and Q. Lin, *ACS Sustainable Chem. Eng.*, 2019, **7**, 11999–12007.

23 L. Lan, T. Li, T. Wei, H. Pang, T. Sun, E. Wang, H. Liu and Q. Niu, *Spectrochim. Acta, Part A*, 2018, **193**, 289–296.

24 (a) P. Rajalakshmi, P. Jayasudha, S. Ciattini, L. Chelazzi and K. P. Elango, *J. Mol. Struct.*, 2019, **1195**, 259–268; (b) M. K. Chahal and M. Sankar, *RSC Adv.*, 2015, **5**, 99028–99036.

25 (a) M. H. Chua, H. Zhou, T. T. Lin, J. Wu and J. Xu, *J. Mater. Chem. C*, 2017, **5**, 12194–12203; (b) M. A. Kaloo and J. Sankar, *Chem. Commun.*, 2015, **51**, 14528–14531.

26 T. M. Ebaston, G. Balamurugan and S. Velmathi, *Anal. Methods*, 2016, **8**, 6909–6915.

27 K. Rezaeian, H. Khanmohammadi and S. Gholizadeh Dogaheh, *New J. Chem.*, 2018, **42**, 2158–2166.

28 (a) M. J. Frisch, G. W. Trucks, H. B. Schlegel, G. E. Scuseria, M. A. Robb, J. R. Cheeseman, and G. Scalmani, *Gaussian 09, Revision D*, Gaussian,Inc, Wallingford, CT, 2013, vol. 1; (b) C. Adamo and D. Jacquemin, *Chem. Soc. Rev.*, 2013, **42**, 845–856.

29 N. S. Karthikeyan, K. I. Sathiyanarayanan and P. G. Aravindan, *Bull. Korean Chem. Soc.*, 2009, **30**, 2555–2558.